Supplemental information

Thermally stable phenylethylammonium-based perovskite passivation: spontaneous passivation with phenylethylammonium bis(trifluoromethylsulfonyl)imide during deposition of PTAA for enhancing photovoltaic performance of perovskite solar cells

Naoyuki Nishimura†, Hiroyuki Kanda†, Ryuzi Katoh§, Atsushi Kogo†, Takurou N. Murakami†*

† National Institute of Advanced Industrial Science and Technology (AIST),1-1-1 Higashi, Tsukuba, Ibaraki 305-8565, Japan.

§ College of Engineering, Nihon University, Koriyama, Fukushima 963-8642, Japan

Corresponding Author

Naoyuki Nishimura, E-mail: naoyuki-nishimura@aist.go.jp

1. Morphological and compositional characterization of PSCs

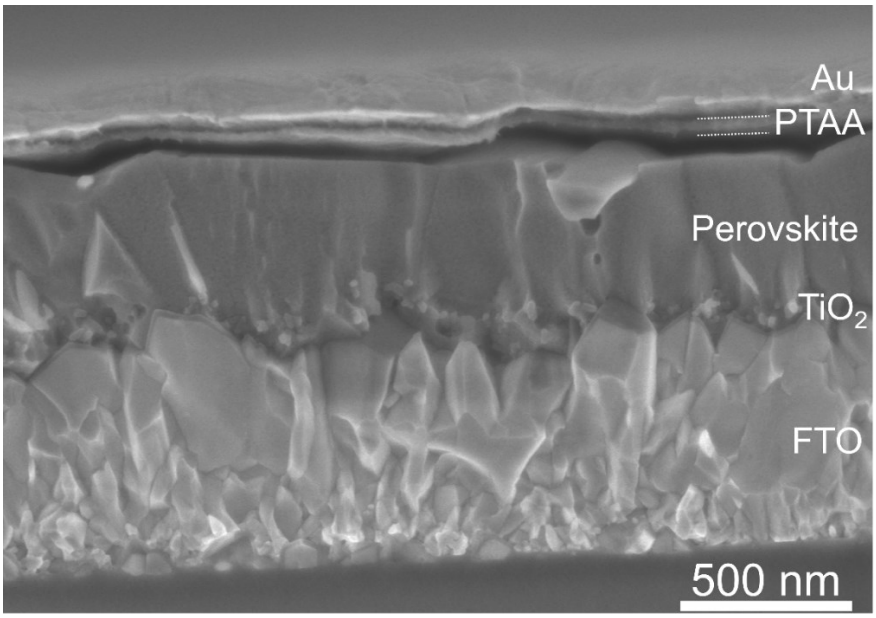

Fig. S1 Cross sectional images of the PSC with Li-TFSI additive

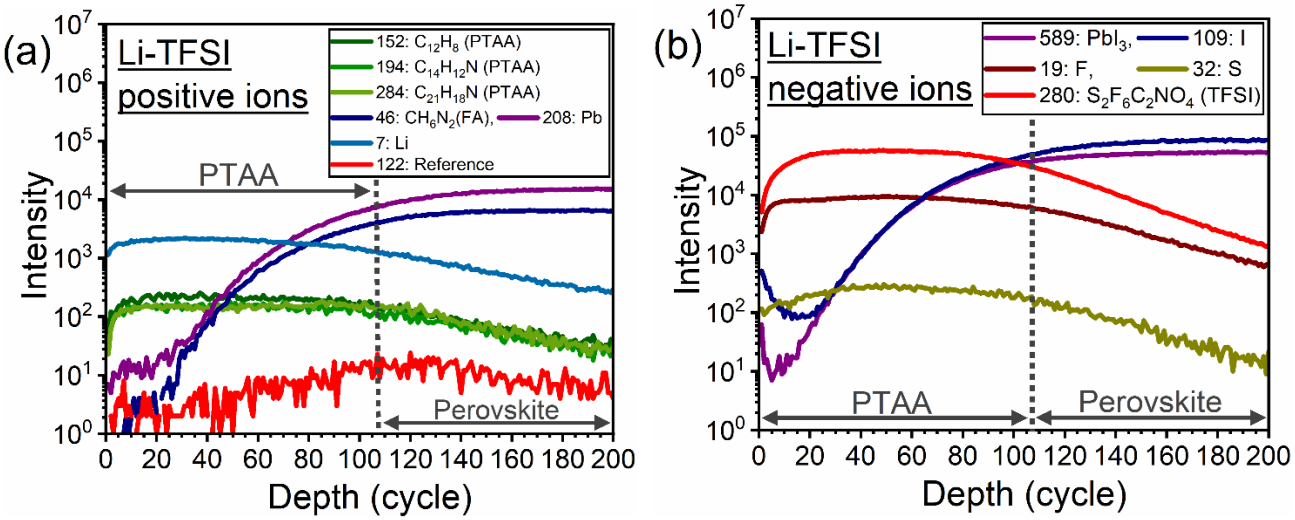

Fig. S2 Results of ToF-SIMS compositional depth analysis of the PTAA/perovskite sample with Li-TFSI (a) positive ions, (b) negative ions

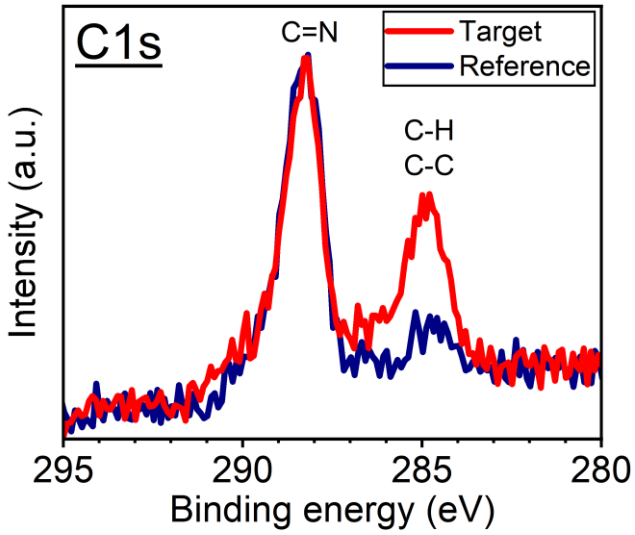

Fig. S3 XPS spectra of perovskite layers

Fig. S3 presents the XPS spectra of the pristine perovskite and the sample after removal of HTM with PEA-TFSI additive. In the spectra of both sample, two peaks at 288.3 eV and around 285 eV corresponding to C=N and C-C + C-H were observed. The sample with PEA-TFSI exhibited a considerably larger peak at 284.5 eV corresponding to C-C and C-H, which was most likely derived from PEA cations.[1] We here note that the small peak at 285 eV observed in the pristine perovskite was presumably originated from contaminated carbons, which generally observed in XPS.

2. PV properties of PCSs

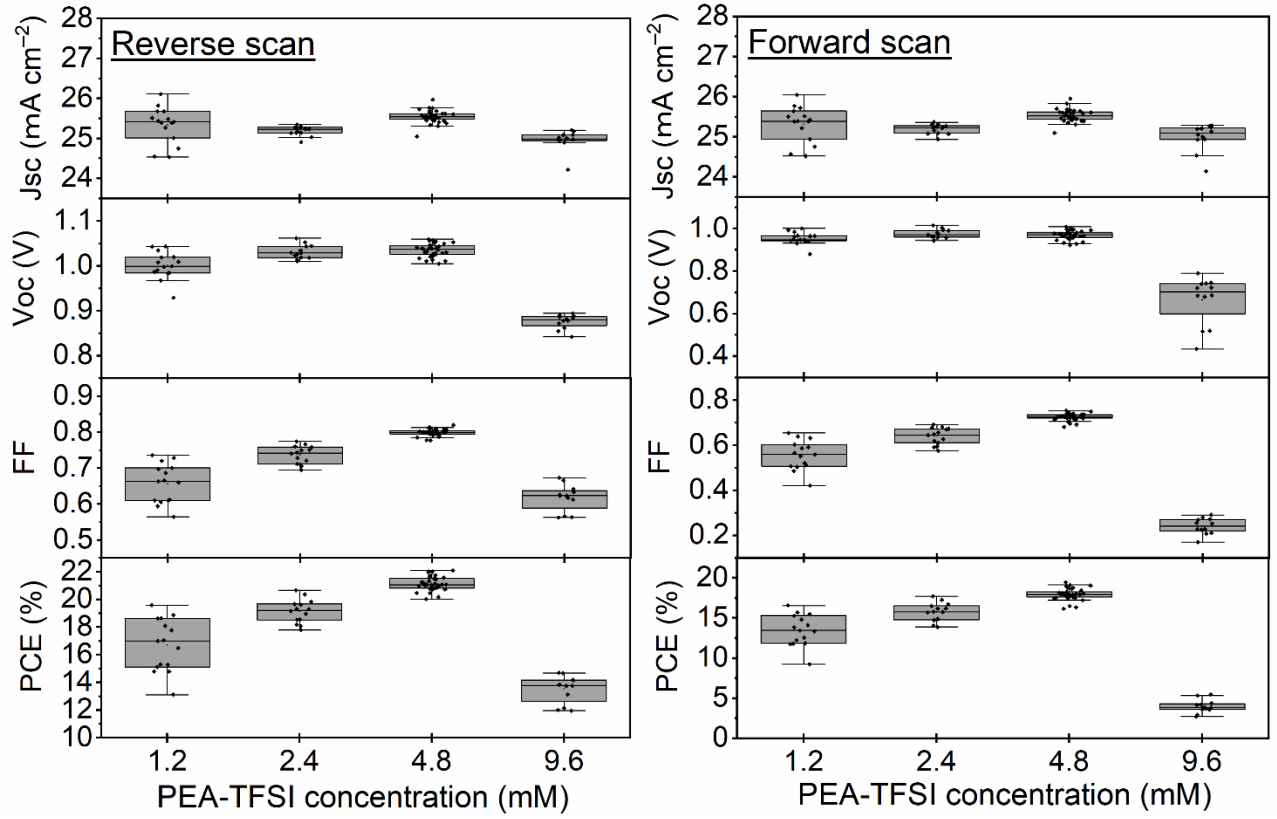

Fig. S4 Optimization of addition amount of PEA-TFSI

Table S1. Averaged PV parameters of PSCs with Li-TFSI and optimal PEA-TFSI

Sample	Scan	Jsc (mA/cm^2)	Voc (V)	FF	η (%)
PEA-TFSI	Backward	25.6 ± 0.2	1.04 ± 0.01	0.80 ± 0.01	21.2 ± 0.5
	Forward	25.5 ± 0.2	0.97 ± 0.02	0.72 ± 0.02	18.0 ± 0.7
Li-TFSI	Backward	25.4 ± 0.3	1.00 ± 0.02	0.74 ± 0.02	18.8 ± 0.9
	Forward	25.4 ± 0.3	0.91 ± 0.03	0.63 ± 0.03	14.5 ± 1.0

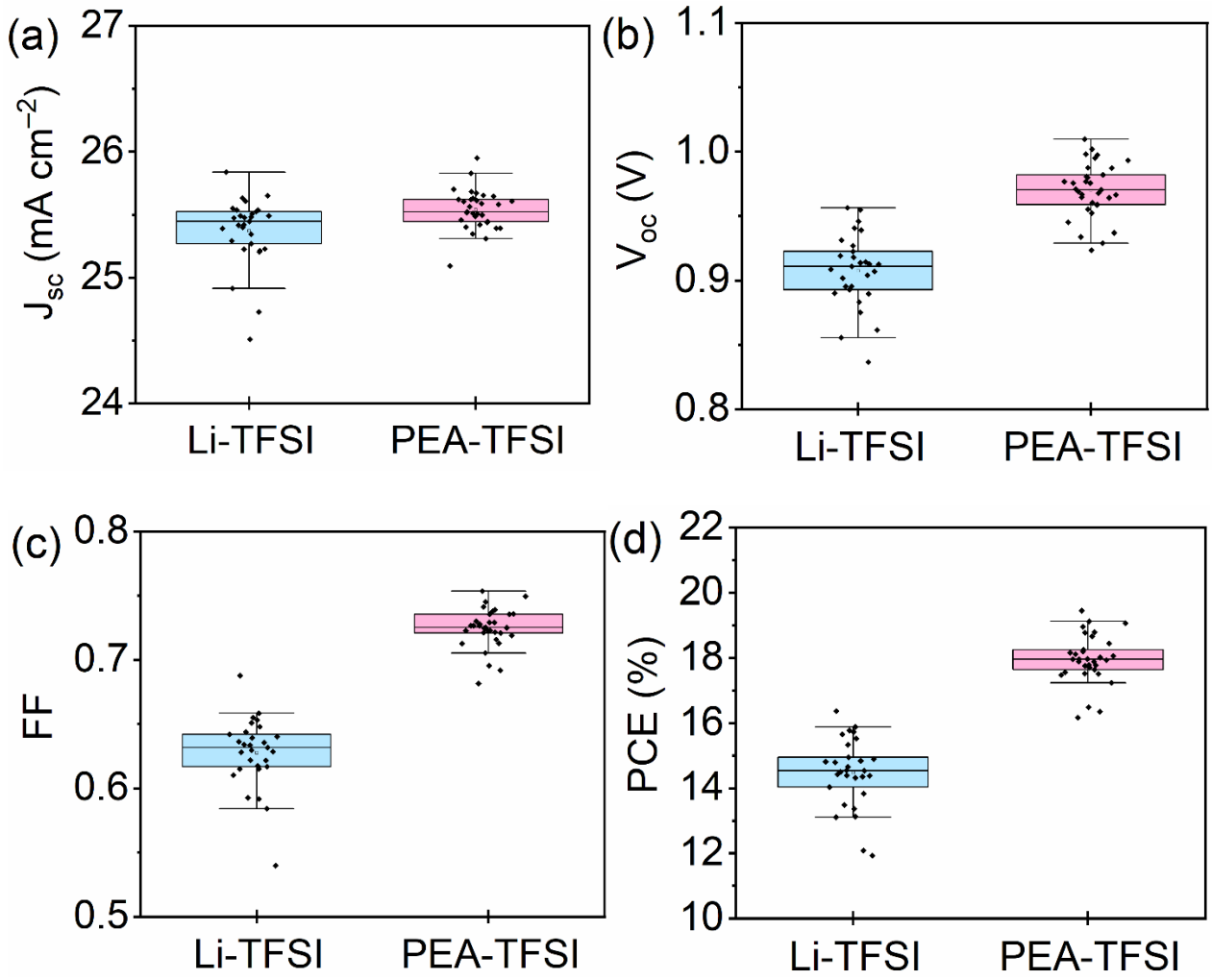

Fig. S5 PV parameter distributions of PSCs with Li-TFSI and PEA-TFSI in forward scan

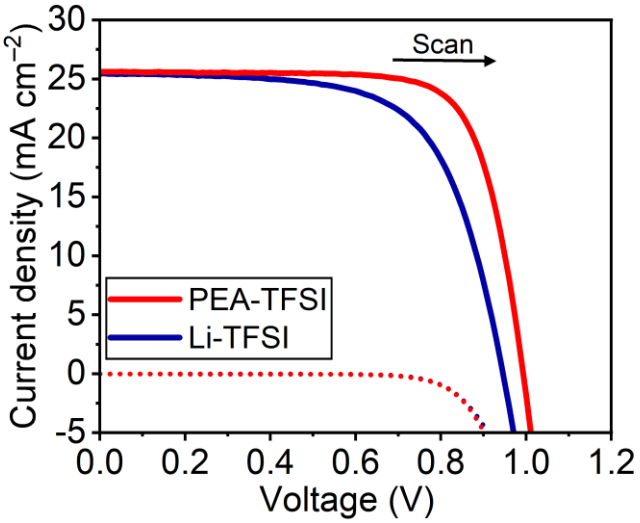

Fig. S6 J-V curves of the best PSCs with Li-TFSI and PEA-TFSI in forward scan

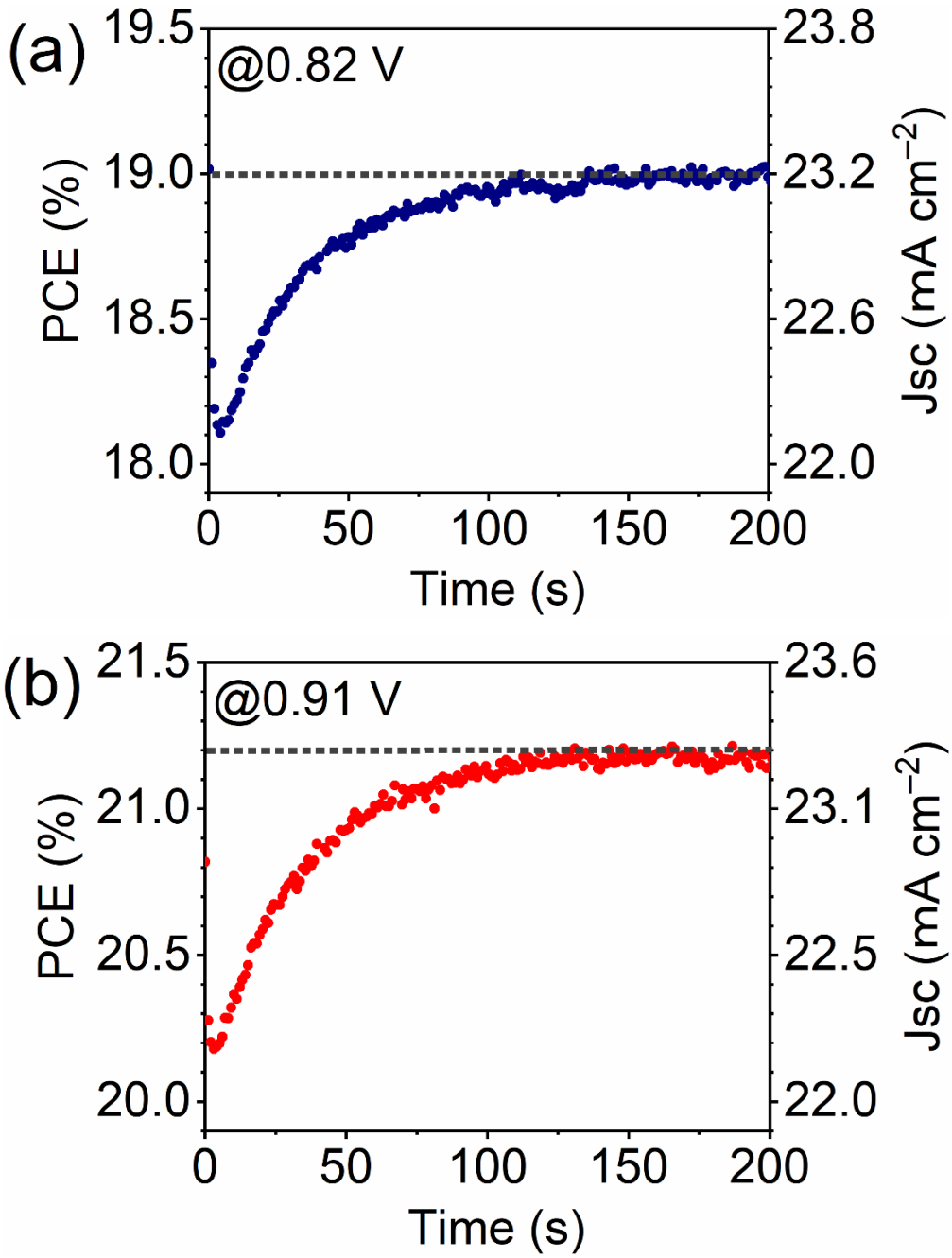

Fig. S7 QSS-PCE of PCSs with (a) Li-TFSI at 0.82 V, and (b) PEA-TFSI at 0.91 V

3. Work functions of PSC materials

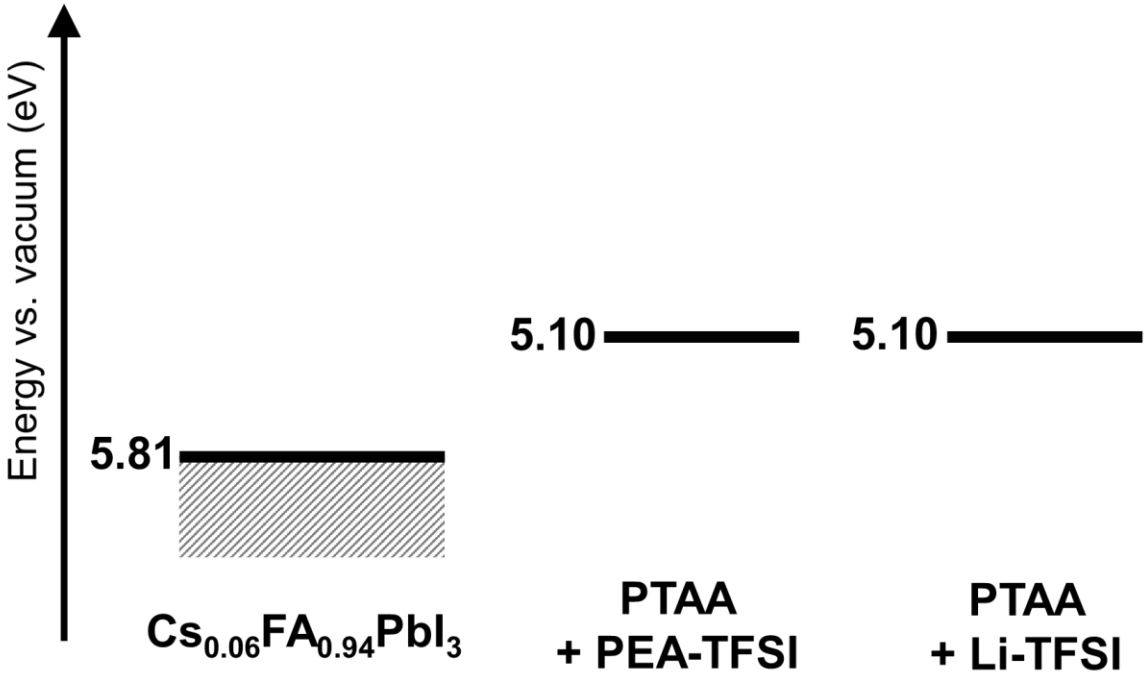

Fig. S8 Energy diagram of work functions of $Cs_{0.06}FA_{0.94}PbI_3$ and PTAA with the optimal PEA-TFSI and Li-TFSI, estimated by PYS measurement

4. Carrier dynamics investigation

TRMC signal ($-\Delta P/P$) is propositional to the following term: [2-8]

$$-\Delta P/P \propto \Phi (\mu_e + \mu_h) \qquad (S1)$$

Here, Φ, μ_e, and μ_h represent yield of free charges, electron mobility, and hole mobility, respectively. Since hole injection of the bilayer samples proceeded sub-ten-ns scale, and μ_e of perovskite is considerably larger than μ_h, TRMC signal decays of the bilayer sample in this work are indicative of electron lifetime in perovskite.[8] Excitation power for Fig. 5b was 0.16 nJ cm^{-2}/ pulse as the decay trend was saturated by this power in the excitation power dependence (Fig. S9) Single exponential fitting for the TRMC decay was employed for the estimation of the electron lifetime.

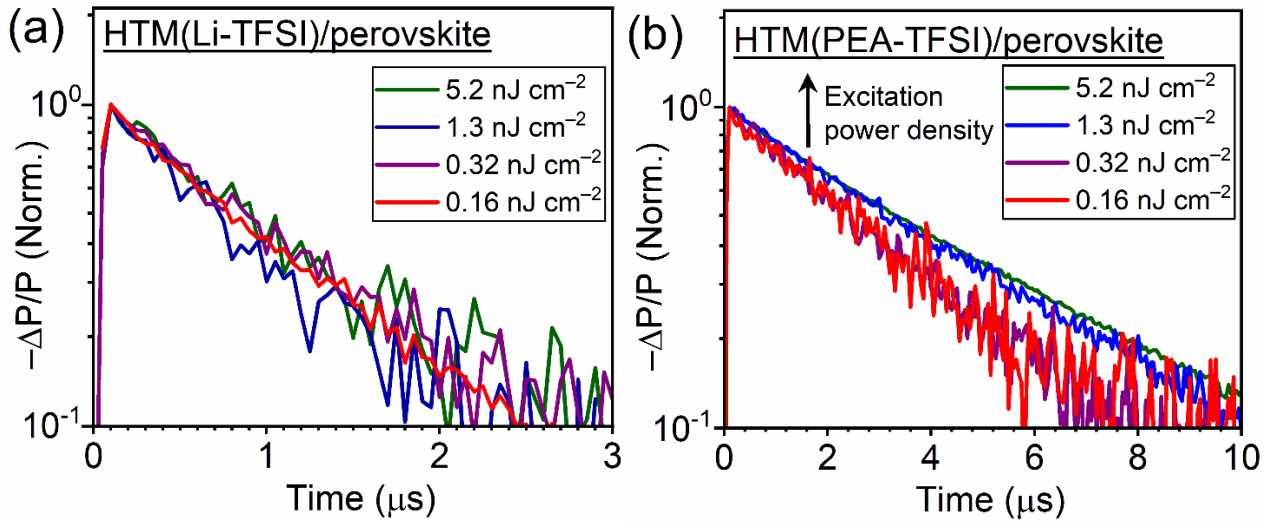

Fig. S9. Excitation intensity dependence on TRMC signals of (a) HTM(Li-TFSI)/ perovskite, (b) HTM(PEA-TFSI)/ perovskite

5. Thermal stability tests

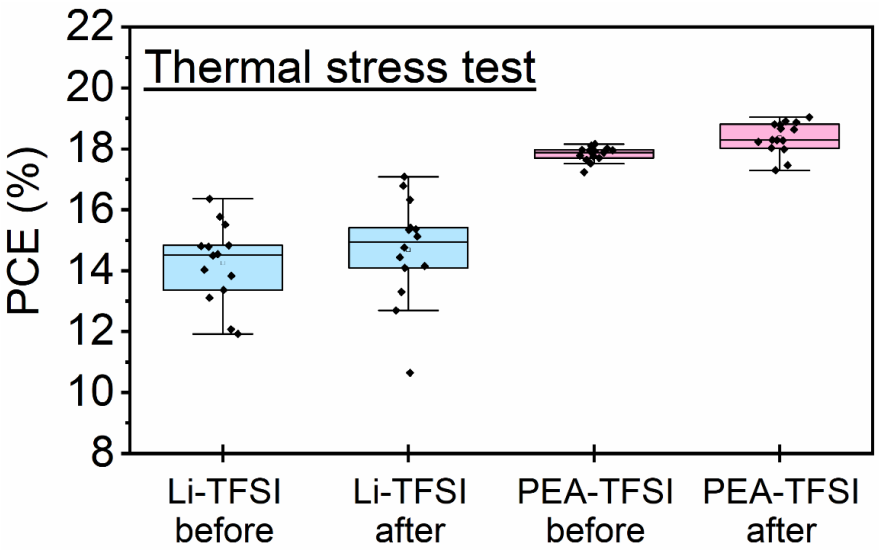

Fig. S10. PCEs of PCSs with Li-TFSI and PEA-TFSI before and after thermal stress at 85℃ for 30 min in N_2 atmosphere in forward scan

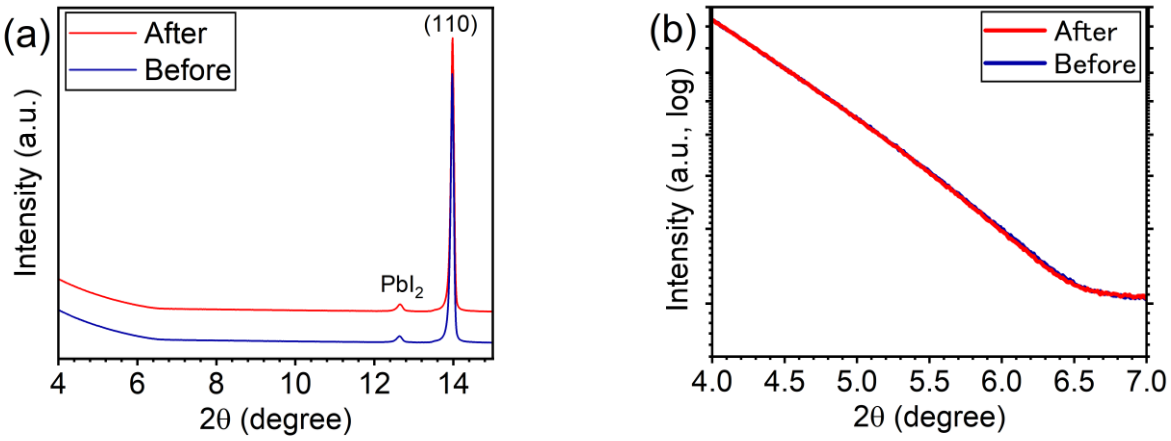

Fig. S11. XRD patterns of the HTM/perovskite sample with PEA-TFSI additive before and after thermal stress at 85℃ for 30 min (a) in a broad scale (b) zoomed in with logarithmic y-axis: no additional diffraction peak after the thermal stress was observed.

6. Problems of OA-based passivation: reduced affinity at the PTAA/perovskite interface

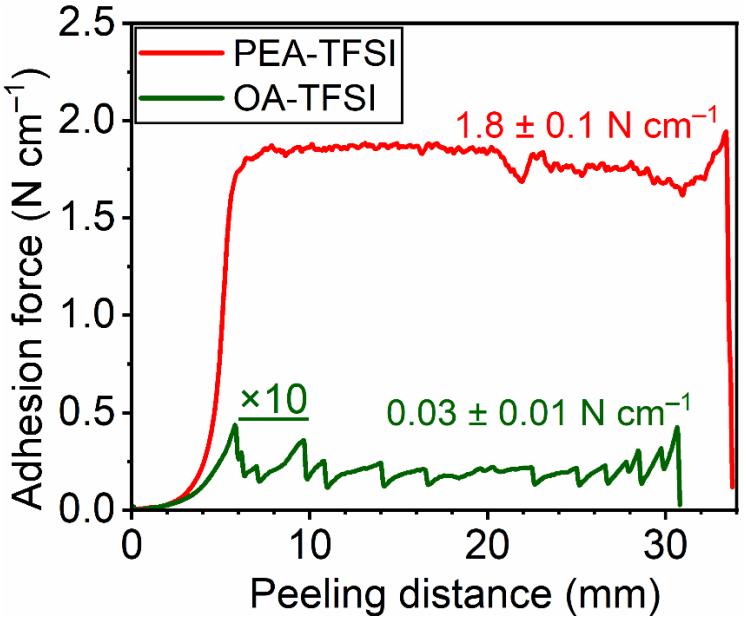

Fig. S12. Results of tape peeling tests for PTAA/perovskite samples with PEA-TFSI and OA-TFSI; the adhesion force of OA-TFSI was magnified by 10 times

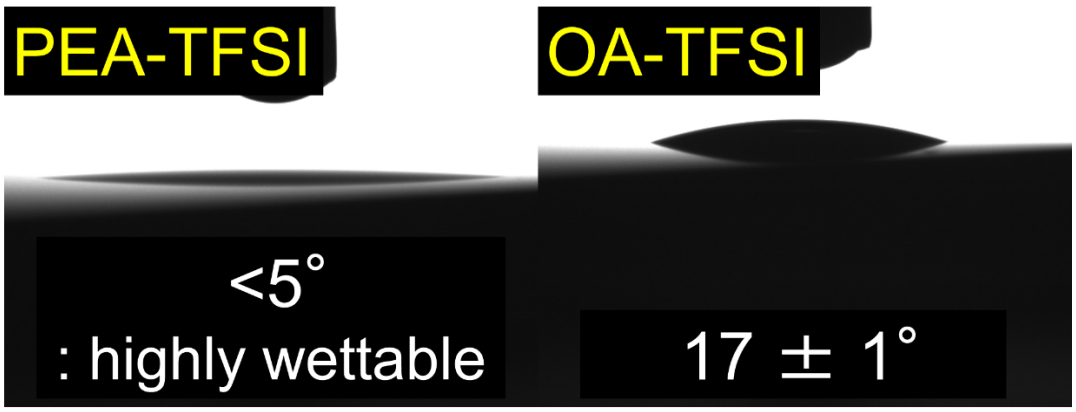

Fig. S13. CA of toluene droplet over perovskite layer after removal of HTM with PEA-TFSI and OA-TFSI

7. Characterization of the synthesized PEA-TFSI

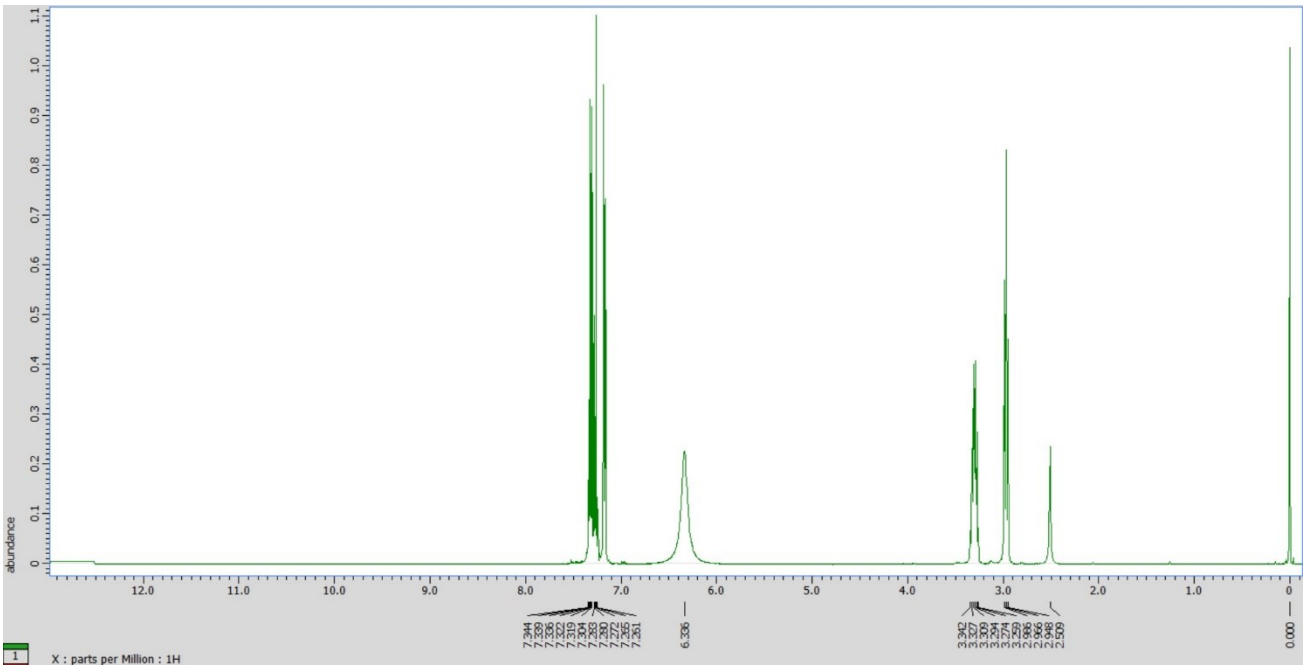

Fig. S14 ^{1}H-NMR spectrum of PEA-TFSI in $CDCl_3$;(400 MHz, $CDCl_3$): δ = 7.16 - 7.34 (m, 5H, Ar), 6.33 (Br, 3H; NH_3), 3.27 - 3.34 (dd, 2H; CH_2NH_3) , 2.94 - 2.98 (t, 2H; $ArCH_2$)

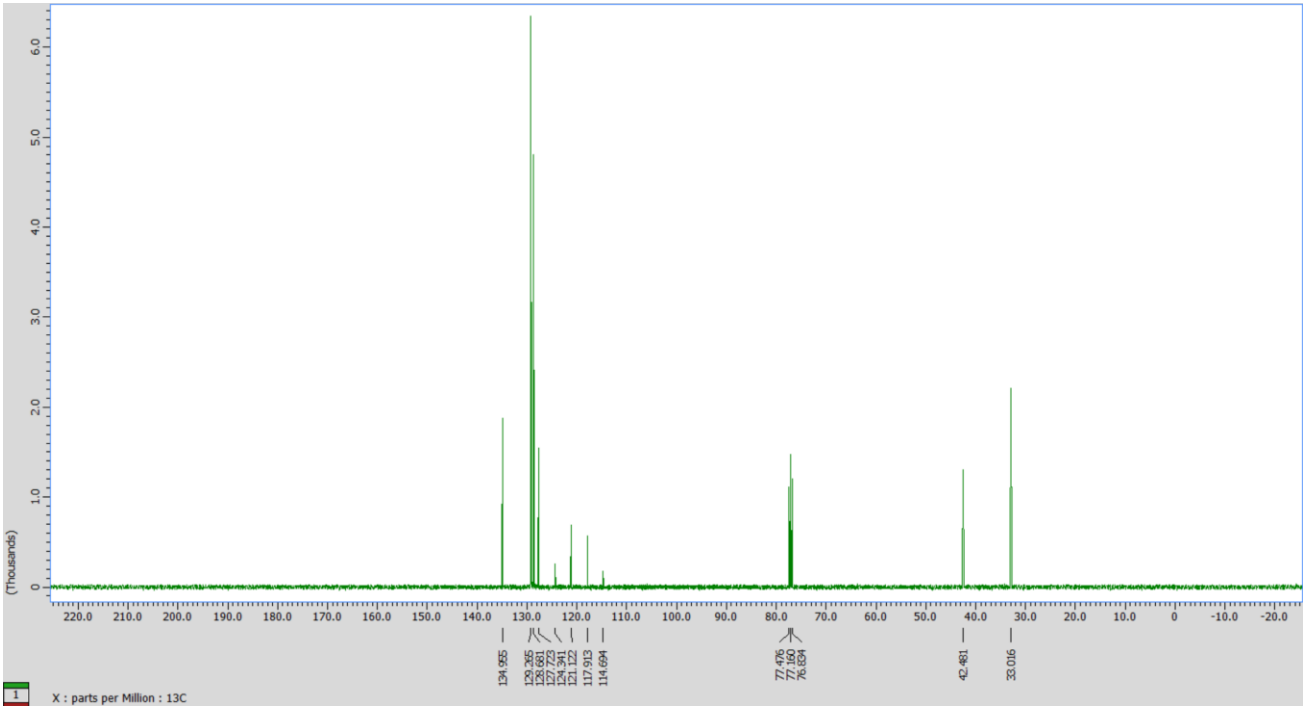

Fig. S15 ^{13}C-NMR spectrum of the synthesized PEA-TFSI in DMSO-d6

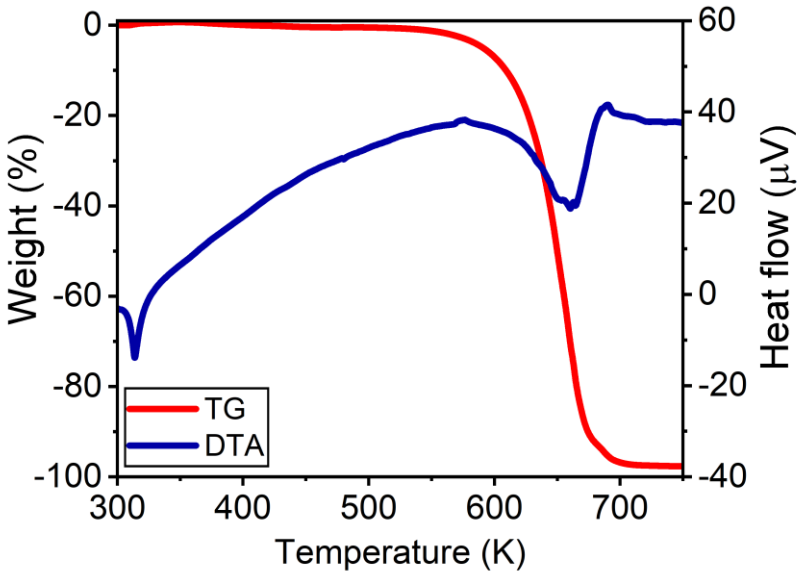

Fig. S16 TG-DTA result of PEA-TFSI under a nitrogen flow

Table S2. Physical properties of PEA-TFSI

Properties	Value
Melting point	314 K
Thermal stability	> 550 K

8. Optical bandgap of photoabsorber material

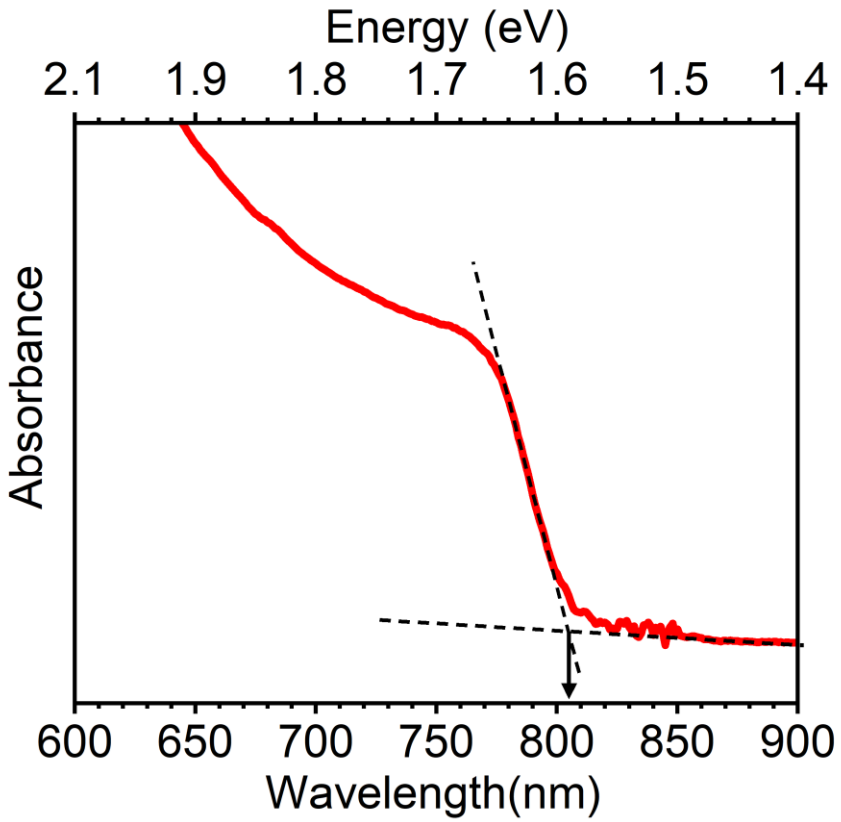

Fig. S17 Absorption spectrum of the photoabsorber layer of $Cs_{0.06}FA_{0.94}PbI_3$; the absorption edge was estimated to be 1.54 eV (805 nm)

Reference

1. Q. Jiang, Y. Zhao, X. Zhang, X. Yang, Y. Chen, Z. Chu, Q. Ye, X. Li, Z. Yin and J. You, *Nat Photonics*, 2019, **13**, 460-466.
2. R. Katoh, A. Furube, K.-i. Yamanaka and T. Morikawa, *J. Phys. Chem. Lett.*, 2010, **1**, 3261-3265.
3. S. Nakajima and R. Katoh, *J. Mater. Chem. A*, 2015, **3**, 15466-15472.
4. H. Oga, A. Saeki, Y. Ogomi, S. Hayase and S. Seki, *J. Am. Chem. Soc.*, 2014, **136**, 13818-13825..
5. E. M. Hutter, J. J. Hofman, M. L. Petrus, M. Moes, R. D. Abellón, P. Docampo and T. J. Savenije, *Adv. Ener. Mater.*, 2017, **7**, 1602349.
6. M. L. Petrus, K. Schutt, M. T. Sirtl, E. M. Hutter, A. C. Closs, J. M. Ball, J. C. Bijleveld, A. Petrozza, T. Bein, T. J. Dingemans, T. J. Savenije, H. Snaith and P. Docampo, *Adv. Ener. Mater.*, 2018, **8**, 1801605.
7. H. Hempel, T. J. Savenjie, M. Stolterfoht, J. Neu, M. Failla, V. C. Paingad, P. Kužel, E. J. Heilweil, J. A. Spies, M. Schleuning, J. Zhao, D. Friedrich, K. Schwarzburg, L. D. A. Siebbeles, P. Dörflinger, V. Dyakonov, R. Katoh, M. J. Hong, J. G. Labram, M. Monti, E. Butler-Caddle, J. Lloyd-Hughes, M. M. Taheri, J. B. Baxter, T. J. Magnanelli, S. Luo, J. M. Cardon, S. Ardo and T. Unold, *Adv. Ener. Mater.*, 2022, **12**, 2102776.
8. N. Nishimura, H. Tachibana, R. Katoh, H. Kanda and T. N. Murakami, *ACS Appl. Mater. Interfaces*, 2023, **15**, 44859-44866.